

Language-Guided Manipulation with Diffusion Policies and Constrained Inpainting

Ce Hao¹, Kelvin Lin¹, Siyuan Luo¹, Harold Soh^{1,2}

¹Dept. of Computer Science, National University of Singapore.

²Smart Systems Institute, NUS.

{cehao, klin-zw, t0933178, harold}@comp.nus.edu.sg

Abstract: Diffusion policies have demonstrated robust performance in generative modeling, prompting their application in robotic manipulation controlled via language descriptions. In this paper, we introduce a zero-shot, open-vocabulary diffusion policy method for robot manipulation. Using Vision-Language Models (VLMs), our method transforms linguistic task descriptions into actionable keyframes in 3D space. These keyframes serve to guide the diffusion process via inpainting. However, naively enforcing the diffusion process to adhere to the generated keyframes is problematic: the keyframes from the VLMs may be incorrect and lead to out-of-distribution (OOD) action sequences where the diffusion model performs poorly. To address these challenges, we develop an inpainting optimization strategy that balances adherence to the keyframes v.s. the training data distribution. Experimental evaluations demonstrate that our approach surpasses the performance of traditional fine-tuned language-conditioned methods in both simulated and real-world settings.

Keywords: Diffusion Policy, Zero-shot Transferring, Inpainting

1 Introduction

Robot manipulation has long been a challenging problem due to the complexity of handling diverse objects in varying contexts. Recent work that applies expressive diffusion models as policies for robot manipulation has enabled the successful reproduction of multi-modal, long-horizon, and multi-object tasks [1, 2, 3, 4, 5, 6].

A crucial extension is to control diffusion policies with language descriptions — this enables use of the unconditional policy for specific contexts via language-conditioning [7, 8, 9, 10]. Current methods train a fine-tuned language-conditioned classifier and modify the gradient during the diffusion process to adjust actions according to task instructions [11, 12, 13, 14]. However, fine-tuned language-conditioned policies typically struggle with unseen tasks and open-vocabulary descriptions [11, 15, 16]. These out-of-distribution (OOD) issues are evident in tasks such as object grasping, where despite training on a large multi-modal dataset, the policies yield incorrect grasps when faced with novel language specifications [17, 18, 19, 20].

To address these challenges, we propose a zero-shot language-guided diffusion policy method using VLM-inspired inpainting optimization (Figure. 1) [21, 22, 23]. Our key idea is that by integrating VLM-generated *keyframes* as actionable guides in a diffusion process, we can bridge the gap between high-level linguistic instructions and low-level robot actions [9, 24, 25]. First, we use a general VLM model (e.g., ChatGPT4) to convert task descriptions into keyframes in 3D space [24]; these keyframes are desired points of action [26, 17]. Then, we employ an inpainting method that uses these keyframes to guide the policy’s action sequence generation [23, 27]. However, our preliminary experiments showed that the standard inpainting method can fail to generate successful trajectories; this occurs when the keyframes are inaccurate or far outside the support of the training distribution [28]. To further enhance robustness in these OOD scenarios, we propose an inpainting

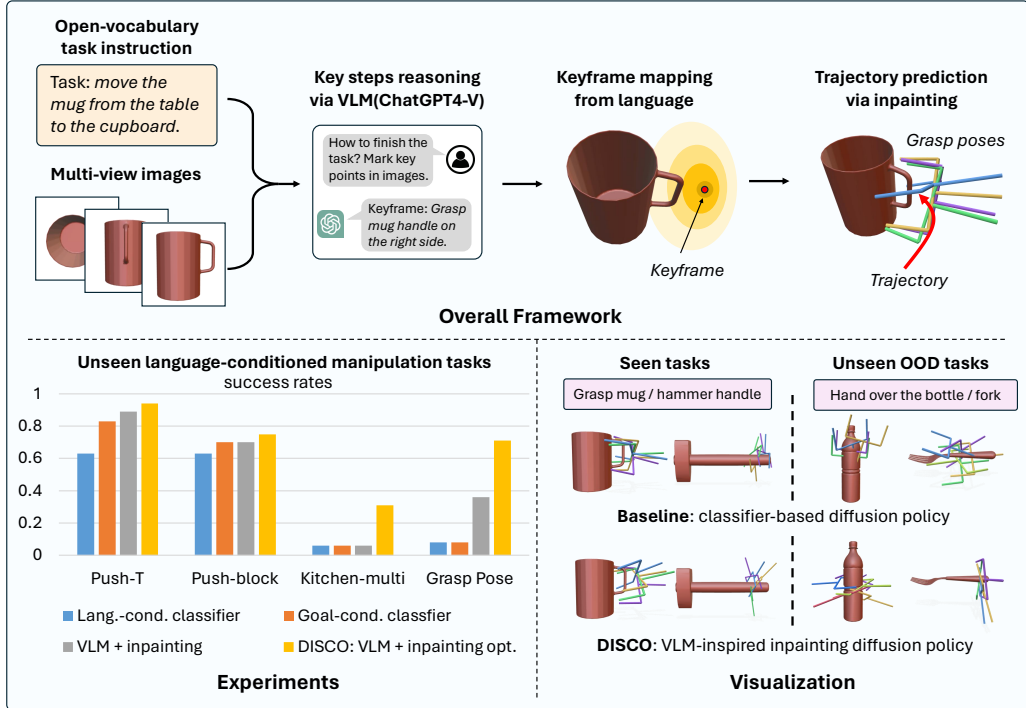


Figure 1: **Overall Framework.** This work proposes a method for zero-shot language-guided diffusion for robot manipulation. Our method, DISCO (Diffusion Inpainting with Semantic Keyframes and Constrained Optimization), uses VLMs (e.g. ChatGPT4-V) to interpret task descriptions and multi-view observations, and generate key steps. These steps are converted into keyframes in 3D space, which then guides the generation of trajectories and grasp poses through constrained inpainting optimization. **Experiments** show our method outperforms language-conditioned and goal-conditioned baselines in new tasks. It also surpasses vanilla inpainting methods in unseen out-of-distribution conditions. **Visualization** shows grasp poses for four objects. Both methods succeeded in known tasks, but our VLM-based approach better generalizes to new open-vocabulary tasks.

optimization method that constrains the generated points to lie within regions of sufficient support during diffusion. This approach balances keyframe adherence and remaining within the support of the diffusion model, which results in better performance for novel or ambiguous task descriptions.

We validate our open-vocabulary diffusion policy — which we call **DISCO** (Diffusion Inpainting with Semantic Keyframes and Constrained Optimization) — using simulated and real-robot experiments [29, 30, 31]. The simulation experiments require generating continuous actions (end-effector positions or velocities) and grasp poses. The tasks involve long-horizon trajectory planning in multi-task environments [32, 33]. Experiments show that in seen tasks, our method achieves comparable performance to fine-tuned language-conditioned policies. In unseen tasks, DISCO obtains significantly higher success rates. These conclusions were supported by our real-world language-guided grasping experiments.

In summary, the contribution of this paper is threefold:

- DISCO, a zero-shot open-vocabulary diffusion policy method that permits language-conditioning via keyframes;
- An constrained inpainting optimization method which circumvents failures due to out-of-distribution keyframes;
- Experimental results on simulated and real robots that validates DISCO’s performance relative to baselines.

2 Method

This section describes our key contribution for zero-shot language-conditioned diffusion. We first provide a problem statement (Sec. 2.1), followed by the key components that make up DISCO. We introduce the keyframe generation method (Sec. 2.2) followed by the inpainting method (Sec. 2.3). We then propose a constrained inpainting optimization (Sec. 2.3) to address the out-of-distribution issues that arise due to poor/invalid keyframes generated by open-vocabulary descriptions.

2.1 Problem Statement

We define the language-conditioned manipulation task as controlling the robot with actions to manipulate objects to achieve a target state under a language specification (or task description) l . The language specifications are “open-vocabulary” in that they contain words and phrases in natural language, beyond a small closed set of labels. The behavior of the robot should comply with the specification. In this work, we have access to image observations O of the robot and objects. The set of observations are assumed to be sufficient to complete the task; for example, multiple views may be available to provide sufficient state information. We seek a policy π that, at each time step t , generates an action (sequence) conditioned on an observation O_t and language description l , i.e., $\mathbf{a}_t \sim \pi(\mathbf{a}_t|O_t, l)$. The task is deemed successful when the target is reached and the robot trajectories satisfy the language specifications.

2.2 Keyframe Generation from Open-Vocabulary Language Descriptions

As illustrated in Figure 1, we employ general multi-modal vision-language models (VLMs), such as ChatGPT4, to analyze the task description l and observation O , and generate action keyframes by:

1. **Delineating the key steps** necessary to complete the task [22, 21]. For example, given the task “Avoid the can and pick up the mug”, the VLM generates two key steps: “First move to the mug from the right side of the can” then “Grasp the mug handle and lift it.”
2. **Mapping key points \mathbf{p}^{key}** on the observations O . We ask the VLMs to map corresponding key points \mathbf{p}^{key} based on the above steps by marking the relevant pixels on the images O . For example, grasping the mug handle would involve marking the handle region. Note that the points marked by VLMs are not exact grasp points (unlike [17, 18, 24]) and cannot be used to directly plan manipulation trajectories. Instead, they serve to provide “coarse” information that guides trajectory generation.
3. **Generating action keyframes \mathbf{a}^{key}** in the environment. Given the key points of the end-effector, we convert them to the keyframes \mathbf{a}^{key} based on the policy and environment. Depending on the exact application, \mathbf{a}^{key} could represent the 3D position, velocity of end-effectors, or robot configuration in joint space.

2.3 Conditional Diffusion Policy via Inpainting

After generating the keyframes \mathbf{a}^{key} , we employ inpainting to perform zero-shot conditional diffusion $\mathbf{a}_t \sim \pi(O_t, \mathbf{a}^{\text{key}})$. Inpainting [34, 35] was originally formulated for image generation, where part of an image is known $\mathbf{x}^{\text{known}}$ and the other part is “masked” (or unknown) $\mathbf{x}^{\text{unknown}}$. Standard inpainting integrates the $\mathbf{x}^{\text{known}}$ and $\mathbf{x}^{\text{unknown}}$ during the reverse step [23],

$$\mathbf{x}_{i-1}^{\text{known}} \sim p_{i-1}^{\text{known}} = \mathcal{N}(\sqrt{\bar{\alpha}_t} \mathbf{x}_0^{\text{known}}, (1 - \bar{\alpha}) I), \quad (1)$$

$$\mathbf{x}_{i-1}^{\text{unknown}} \sim q_{i-1}^{\text{unknown}} = \mathcal{N}(\mu_\theta(\mathbf{x}_i, i), \Sigma_\theta(\mathbf{x}_i, i)), \quad (2)$$

$$\mathbf{x}_{i-1} = \mathbf{m} \odot \mathbf{x}_{i-1}^{\text{known}} + (1 - \mathbf{m}) \odot \mathbf{x}_{i-1}^{\text{unknown}}. \quad (3)$$

In Eqn. (1) and (2), $\mathbf{x}_{i-1}^{\text{known}}$ and $\mathbf{x}_{i-1}^{\text{unknown}}$ denote the known part of the image and the unknown inpainting parts, sampled from the probabilities p_{i-1}^{known} and q_{i-1}^{unknown} at $(i-1)$ th step. $\bar{\alpha}$, μ_θ and Σ_θ represent the scheduling parameters and parameters of the learned diffusion distribution, respectively [23, 36]. \mathbf{m} represents the inpainting mask, which takes a value of 1 for known and 0 for unknown regions.

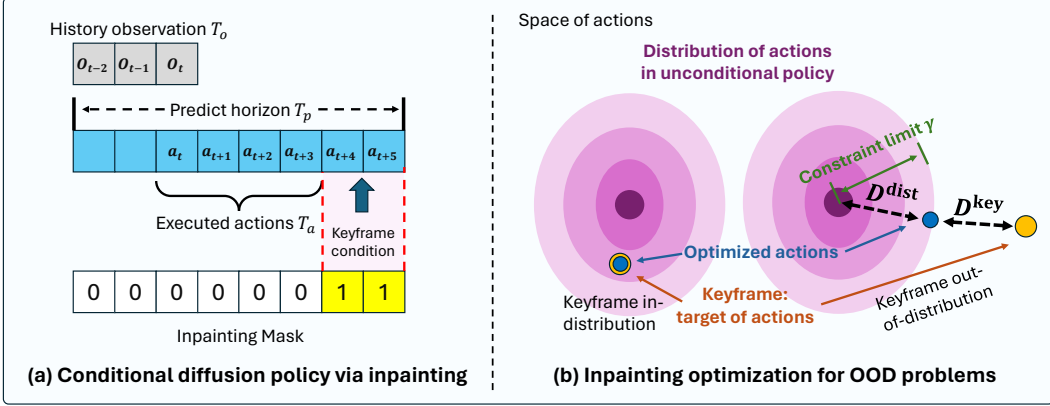


Figure 2: **(a)**: Inpainting controls the trajectory generation of diffusion policy via keyframes. **(b)**: Our inpainting optimization method constrains the generated actions to lie within regions of sufficient support (high likelihood). D^{dist} represents the negative log-likelihood constraint in Eqn. (5).

During the reverse diffusion step, \mathbf{x}_{i-1} is constructed by merging the masked $\mathbf{x}_{i-1}^{\text{known}}$ and $\mathbf{x}_{i-1}^{\text{unknown}}$. This integration ensures that the content generated for the unknown regions is conditioned on the known regions, leading to a coherent output.

In this paper, we apply inpainting to diffusing policies in combination with receding-horizon control [2]. As illustrated in Figure 2(a), at time t , the diffusion policy utilizes historical observations O_t with length T_o to generate a predicted multi-step action sequence a_t with length T_p , and executes the first T_a actions. At time $t + T_a$, the policy enters the next cycle, repeating the observation and trajectory generation until the task is completed. During the generation of the action sequence, inpainting is applied by setting the known part as the keyframes, i.e., $\mathbf{x}_0^{\text{known}} = \mathbf{a}^{\text{key}} \cdot \mathbf{m}$. In this setup, the mask \mathbf{m} for the first $T_o + T_a - 1$ steps is set to 0, and subsequent steps are set to 1. Thus, \mathbf{a}^{key} serves to condition the generation of $\mathbf{x}^{\text{unknown}}$. When one task contains multiple keyframes, we sequentially select each keyframe and apply inpainting to complete each sub-task.

2.4 Inpainting Optimization for Out-of-Distribution Keyframes

When the keyframe falls within the distribution of the diffusion model, the generated action sequence typically leads to successful task completion. However, when the keyframe is out-of-distribution (OOD), vanilla inpainting forces the generation to comply with the OOD keyframe which leads to poor generation of $\mathbf{x}^{\text{unknown}}$. This causes the entire action sequence to be OOD, which results in the robot state moving towards regions that are not well supported by the training data. Consequently, the behavior produced by the policy fails to accomplish the task.

To address these issues, we propose a constrained inpainting optimization approach. Intuitively, we adjust the generation process to ensure that even when faced with OOD keyframes, the generated action sequences remain within the data distribution. This approach helps sustain task performance even under the challenging conditions introduced by novel task descriptions. More formally, during the reverse step of the diffusion model, we replace Eqn. (3) with,

$$\mathbf{x}_{i-1} = \arg \min_{\mathbf{x}_{i-1}} D^{\text{key}}(\mathbf{m} \odot \mathbf{x}_{i-1}^{\text{known}}, \mathbf{m} \odot \mathbf{x}_{i-1}), \quad (4)$$

$$\text{s.t. } -\log(q_{i-1}^{\text{unknown}}(\mathbf{x}_{i-1})) \leq \gamma_{i-1}, \quad (5)$$

where, $\mathbf{x}_{i-1}^{\text{known}}$ denotes the known part in Eqn. (1) and q_{i-1}^{unknown} is density in Eqn. (2). D^{key} measures the distance between the generated \mathbf{x}_{i-1} and the $\mathbf{x}_{i-1}^{\text{known}}$ (keyframe). We design the distance function D^{key} according to the policy and task environment. In this work, we use L2-norm as D^{key} for actions in 3D space. We constrain the negative log-likelihood $-\log(q_{i-1}^{\text{unknown}}(\mathbf{x}_{i-1}))$ to be bounded by hyperparameter γ_i

In Figure 2 (b), we illustrate the process of inpainting optimization. The left diagram shows that the keyframe is within a high-likelihood region of $p(\mathbf{x}_{i-1}^{\text{known}})$, i.e., $-\log(q_{i-1}^{\text{unknown}}(\mathbf{x}_{i-1})) \leq \gamma_{i-1}$. In this scenario, inequality Eqn. (5) is always satisfied, and thus the formula reduces to vanilla inpainting (Eqn. (3)). In the right diagram, since $-\log(q_{i-1}^{\text{unknown}}(\mathbf{x}_{i-1})) \geq \gamma_{i-1}$, constrained optimization via Eqn (5) results in a generated action sequence that lies within the training data distribution but also minimizes the distance to the keyframe. This enables the policy to complete the task while maximally satisfying the language specification.

3 Related Works

Language-conditioned robot manipulation, where natural language is used to guide robot behavior, has been receiving increased attention, partially due to the advances made in large-language models. One line of prior work has applied vision-language models (VLMs) to convert linguistic descriptions into executable trajectories [7, 11, 21, 22]. Other methods use VLMs to transform language descriptions into code, affordances, and actionable trajectory tokens [16, 37, 18, 25]. Despite their versatility, VLM-based policies often struggle with tasks that require high precision, primarily due to the inherent multi-modal nature of demonstrations, which can lead to ambiguous or conflicting interpretations of the language commands [38, 10]. To address this issue, our method introduces keyframes as an intermediate representation to bridge high-level language commands and low-level trajectories [24, 20].

Diffusion-based policies are a rich policy class that can represent multi-modal and high-dimensional action distributions. They have been shown to be excellent for imitation learning, where they exhibit intricate and complex motion [2, 4, 6, 29, 3, 5]. Recent advancements have expanded diffusion policy applications to include goal-conditioned and language-conditioned tasks [12, 13, 14], providing a structured approach to integrating explicit objectives and linguistic instructions into action generation [7, 39]. However, these methods typically require extensive fine-tuning for each specific task, limiting their ability to generalize to unseen, open-vocabulary tasks [10, 20, 40]. To tackle this, we propose a zero-shot transfer strategy using inpainting, complemented by constrained optimization to handle out-of-distribution keyframes resulting from novel task descriptions [28, 23].

Inpainting was originally developed for image completion [35], but have been adapted for use with diffusion policies to generate actions rather than images [36, 23]. These methods have been also applied to goal-conditioned planning, using goals as known conditions to guide action generation [41, 27, 4]. In our approach, we apply inpainting within the diffusion policy framework to generate trajectories and grasp poses, employing keyframes as conditions for action sequences [34].

4 Experiments and Analysis

In this section, we describe experiments designed to validate DISCO’s performance. We first describe the language-conditioned simulation environments and baseline methods (Sec. 4.1). Then, we analyze and compare the experimental results in seen and unseen tasks (Sec. 4.2). We also discuss ablation studies to analyze the performance of our inpainting optimization technique (Sec. 4.3). Finally, we transfer the policy from simulation to a real robot and test the Sim2Real generalizability of DISCO (Sec. 4.4).

4.1 Simulation Environments and Baselines

Simulation Environments. As shown in Figure 3, we adapt four environments for language-conditioned manipulation tasks. We generated corresponding language descriptions and subgoals for the action sequences on the dataset. We categorize tasks into “seen tasks” and “unseen tasks” based on the environment and dataset. Seen tasks have language conditions that have appeared in demonstrations, requiring the policy to complete tasks while adhering to these conditions. In contrast, unseen tasks did not exist in the demonstrations. They included new language descriptions for

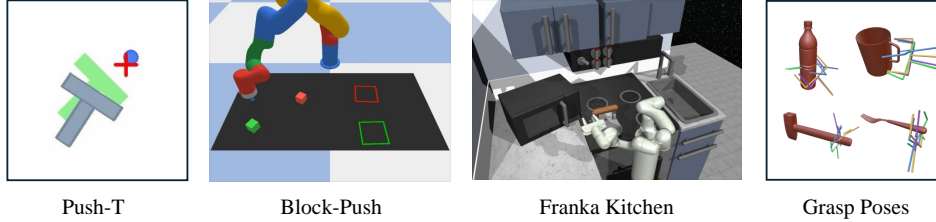


Figure 3: Simulation experimental environments, adapted for language-conditioned tasks. **Push-T** [30]: The robot arm pushes the T-block to a target region, with the added condition that the trajectory passes through the block’s left, right, top, and bottom sides. **Block-push** [31]: The robot arm pushes two differently colored blocks to two targets, with the condition that a specific colored block is pushed to a target in a designated order. **Franka kitchen** [32]: The tasks are divided into single tasks and tasks across three regions (parts of the kitchen). For *single tasks*, we randomly select one region to complete the task, all of which are seen. *Composite/multi tasks* involve two regions and require the robot to complete tasks in the order specified by the condition. **Grasp Pose** generation [33]: We tested the functionality of using language to control the robot gripper to grasp objects, choosing objects like mugs, bottles, hammers, and forks, with various language instructions such as grasping a certain region or simply using the object. In this environment, the policy only generates single grasp poses, so the $T_o = T_p = T_a = 1$ and we directly apply the condition to the single action.

existing behaviors in the demonstration and completely novel tasks beyond the demonstrations. We tested the transferability of different conditional diffusion policies on the unseen tasks.

Baselines. We trained an **unconditional diffusion policy** [2, 33] as the main baseline. We trained fine-tuned **language-conditioned** (Lang.-cond.) [14] classifiers and **goal-conditioned** (Goal-cond.) [13] classifiers and employed classifier-based diffusion models to control the generation of actions. We also conducted comparative tests with **vanilla inpainting** (Vanilla inpt.) [23] to ascertain the potential advantage of constrained inpainting optimization (Inpt. opt.).

4.2 Main Experimental Results

The experimental results are presented in Table 1. In **seen tasks**, the language-conditioned and goal-conditioned classifiers-based diffusion policies achieved high success rates in tasks like push-T, push-block, and Franka kitchen (single task). However, on the Franka kitchen composite tasks

Table 1: Results of Simulation Experiments (success rate \uparrow)

		Push-T	Push-block	Kitchen		Grasp Pose Generation			
				Single	Multi	Mug	Bottle	Ham.	Fork
Seen tasks ¹	No condition	0.54	0.50	0.12	0.03	0.47	0.31	0.40	0.48
	Lang.-cond.	0.98	1.00	1.00	0.31	0.91	0.84	0.78	0.96
	Goal-cond.	0.96	1.00	1.00	0.27	0.88	0.95	0.70	0.93
	Vanilla inpt.	0.82	1.00	0.71	0.35	0.90	0.88	0.85	0.96
	DISCO(ours)	0.87	1.00	0.71	0.42	0.92	0.92	0.97	0.97
Unseen tasks ²	Lang.-cond.	0.63	0.63	-	0.06	0.02	0.04	0.02	0.24
	Goal-cond.	0.83	0.70	-	0.06	0.00	0.08	0.00	0.23
	Vanilla inpt.	0.89	0.70	-	0.06	0.02	0.30	0.58	0.55
	DISCO (ours)	0.94	0.75	-	0.31	0.65	0.51	0.80	0.87

¹ **Seen tasks** appeared in the demonstrations with language descriptions;

² **Unseen tasks** had new language descriptions in addition to the demonstrations. The policies are only trained in the seen demonstrations and zero-shot transferred to unseen tasks.

* Baselines methods are in section 4.1. Success rates are calculated over 50 trials in each task.

and grasp pose generation, vanilla inpainting and DISCO achieved better success rates. On **unseen tasks**, the success rates of the DISCO are significantly higher than the other baseline methods. One potential reason is that the language and goal-conditioned policies failed to generalize to unseen task descriptions. In contrast, inpainting methods leverage the keyframes generated by VLMs which have been trained on large amounts of text data. However, unseen tasks also led to out-of-distribution keyframes that did not appear in the demonstration; this resulted in vanilla inpainting failing to generate successful action trajectories since it enforced strong conformity to the keyframes. DISCO does not suffer from this problem as it applies constrained optimization to keep the action sequences within the support of the generative model.

4.3 Ablation Studies of Inpainting Optimization

Inpainting Optimizaiton v.s. Vanilla Inpainting. We illustrate the improvement of inpainting optimization over vanilla inpainting in a 1D regression example (Figure 4). We generate 1D cubic spline distributions with two modes at $+0.3$ and -0.3 . Then we set three different keyframes as $x^{\text{known}} = 0.7, 0.3$ and 0.1 and apply both inpainting methods. Compared to vanilla inpainting, the distributions resulting from inpainting optimization are significantly closer to the original demonstration distribution.

Inpainting Optimization Constraint. We study the influence of the optimization constraint γ_i in Eqn. (5) on the performance of inpainting optimization. In Figure 5, we vary γ_i in the grasp pose generation tasks, where the keyframes deviate significantly from the demonstrations. When γ_i is relatively small, the generated actions align closely with the unconditional demonstration, achieving successful grasping, but they often fail to meet the specified conditions. As γ_i increases, inpainting optimization compels the actions to satisfy these conditions more rigorously, but this adherence to the keyframes can substantially lower the success rate. Therefore, a moderate γ_i can strike an optimal balance between condition fulfillment and alignment with the demonstration distribution, thereby maximizing the conditional success rate.

4.4 Zero-shot Transfer to Real Robot

We transferred a grasp pose generation model trained in simulation to a real-world Franka Emika robot (Figure 6). We applied DISCO to generate 3D keyframes given real images and point clouds,

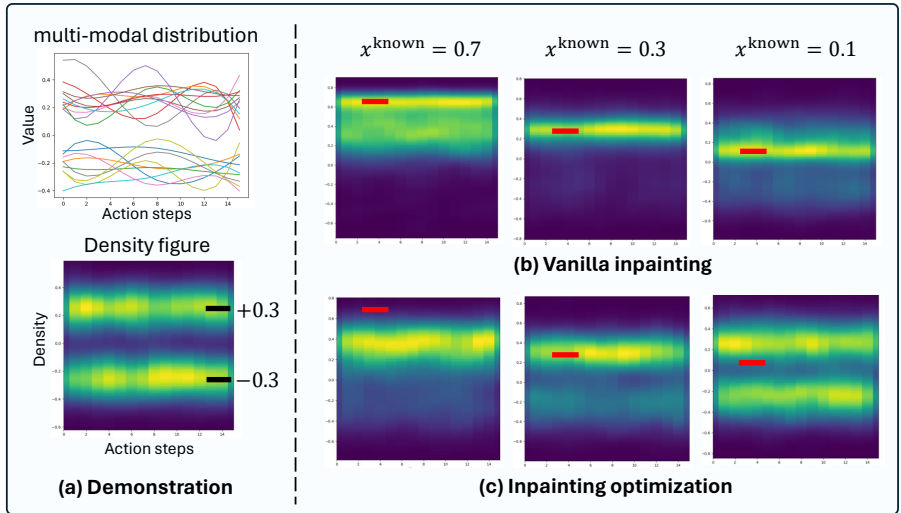


Figure 4: **Illustration of inpainting optimization.** (a) The demonstration has two modes at $+0.3$ and -0.3 (black bar). We set condition x^{known} at $0.7, 0.3$, and 0.1 (red bar) and apply inpainting methods. (b) The vanilla inpainting method fails to align with the demonstration. (c) The inpainting optimization can successfully capture one or two modes based on the known conditions.

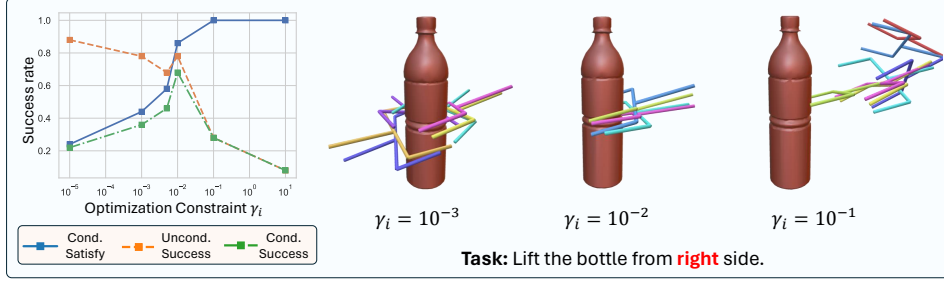


Figure 5: **Ablation study** of inpainting optimization (Eqn. (4), (5)) in grasp pose environment (keyframes omitted in the figures). As the constraint γ_i increases, the generated actions increasingly satisfy the specified conditions. However, excessively high values compromise the overall success of the task. A carefully chosen γ_i balances condition satisfaction against task success.

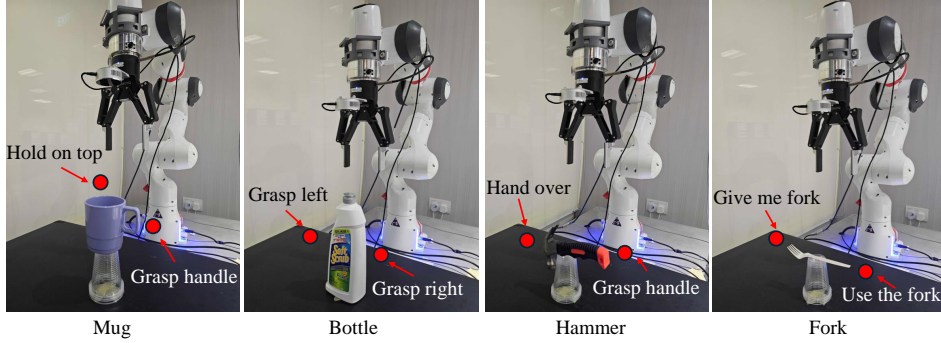


Figure 6: **Real-robot experiments.** We zero-shot transfer the grasp pose generation methods to the real objects with different language instructions.

then generated conditional grasp poses via inpainting optimization. We used a *single* model trained in simulation to generalize across all object categories without any parameter fine-tuning.

We tested each object with seen and unseen tasks in 10 trials. The classifier-based methods achieved only a 6% success rate in seen tasks and 0% in unseen tasks. In contrast, the vanilla inpainting and inpainting optimization methods achieved success rates of 30% to 40% in seen tasks. Notably, while vanilla inpainting faltered in unseen tasks (0%), inpainting optimization maintained a 30% success rate.

5 Conclusion

In conclusion, we propose DISCO, a zero-shot, open-vocabulary framework for robot manipulation using language descriptions. By leveraging VLMs, our method guides diffusion policies through actionable keyframes and addresses critical out-of-distribution issues with an inpainting optimization technique. This approach not only matches but surpasses traditional fine-tuned methods in both simulated and real-world settings. DISCO integrates natural language processing with robot control, thus supporting more complex interactions in varied environments.

Limitations and Future Work. There are several improvements that can be made to DISCO. At present, inpainting cannot be used to control objects other than the robot. Moreover, in multi-task environments, a single keyframe may be associated with multiple objects, potentially resulting in incorrect manipulation or entrapment in the intersection of multiple operational modes. Future work should focus on developing diffusion policies that can simultaneously predict the states of objects and the actions of the robot. This would allow inpainting methods to more effectively condition on the specific states of target objects.

References

- [1] O. Mees, L. Hermann, E. Rosete-Beas, and W. Burgard. Calvin: A benchmark for language-conditioned policy learning for long-horizon robot manipulation tasks. *IEEE Robotics and Automation Letters*, 7(3):7327–7334, 2022.
- [2] C. Chi, S. Feng, Y. Du, Z. Xu, E. Cousineau, B. Burchfiel, and S. Song. Diffusion policy: Visuomotor policy learning via action diffusion. *arXiv preprint arXiv:2303.04137*, 2023.
- [3] Y. Ze, G. Zhang, K. Zhang, C. Hu, M. Wang, and H. Xu. 3d diffusion policy. *arXiv preprint arXiv:2403.03954*, 2024.
- [4] M. Janner, Y. Du, J. B. Tenenbaum, and S. Levine. Planning with diffusion for flexible behavior synthesis. *arXiv preprint arXiv:2205.09991*, 2022.
- [5] Z. Xian, N. Gkanatsios, T. Gervet, T.-W. Ke, and K. Fragkiadaki. Chaineddiffuser: Unifying trajectory diffusion and keypose prediction for robotic manipulation. In *7th Annual Conference on Robot Learning*, 2023.
- [6] X. Li, V. Belagali, J. Shang, and M. S. Ryoo. Crossway diffusion: Improving diffusion-based visuomotor policy via self-supervised learning. *arXiv preprint arXiv:2307.01849*, 2023.
- [7] H. Zhou, X. Yao, Y. Meng, S. Sun, Z. Bing, K. Huang, and A. Knoll. Language-conditioned learning for robotic manipulation: A survey. *arXiv preprint arXiv:2312.10807*, 2023.
- [8] J. Wu, R. Antonova, A. Kan, M. Lepert, A. Zeng, S. Song, J. Bohg, S. Rusinkiewicz, and T. Funkhouser. Tidybot: Personalized robot assistance with large language models. *Autonomous Robots*, 47(8):1087–1102, 2023.
- [9] K. Rana, J. Haviland, S. Garg, J. Abou-Chakra, I. Reid, and N. Suenderhauf. Sayplan: Grounding large language models using 3d scene graphs for scalable task planning. *arXiv preprint arXiv:2307.06135*, 2023.
- [10] M. Ahn, A. Brohan, N. Brown, Y. Chebotar, O. Cortes, B. David, C. Finn, C. Fu, K. Gopalakrishnan, K. Hausman, et al. Do as i can, not as i say: Grounding language in robotic affordances. *arXiv preprint arXiv:2204.01691*, 2022.
- [11] S. Stepputtis, J. Campbell, M. Phielipp, S. Lee, C. Baral, and H. Ben Amor. Language-conditioned imitation learning for robot manipulation tasks. *Advances in Neural Information Processing Systems*, 33:13139–13150, 2020.
- [12] J. Ho and T. Salimans. Classifier-free diffusion guidance. *arXiv preprint arXiv:2207.12598*, 2022.
- [13] M. Reuss, M. Li, X. Jia, and R. Lioutikov. Goal-conditioned imitation learning using score-based diffusion policies. *arXiv preprint arXiv:2304.02532*, 2023.
- [14] H. Ha, P. Florence, and S. Song. Scaling up and distilling down: Language-guided robot skill acquisition. In *Conference on Robot Learning*, pages 3766–3777. PMLR, 2023.
- [15] F. Liu, K. Fang, P. Abbeel, and S. Levine. Moka: Open-vocabulary robotic manipulation through mark-based visual prompting. *arXiv preprint arXiv:2403.03174*, 2024.
- [16] A. Brohan, N. Brown, J. Carbajal, Y. Chebotar, J. Dabis, C. Finn, K. Gopalakrishnan, K. Hausman, A. Herzog, J. Hsu, et al. Rt-1: Robotics transformer for real-world control at scale. *arXiv preprint arXiv:2212.06817*, 2022.
- [17] M. Shridhar, L. Manuelli, and D. Fox. Cliport: What and where pathways for robotic manipulation. In *Conference on robot learning*, pages 894–906. PMLR, 2022.

- [18] M. Shridhar, L. Manuelli, and D. Fox. Perceiver-actor: A multi-task transformer for robotic manipulation. In *Conference on Robot Learning*, pages 785–799. PMLR, 2023.
- [19] K. Lin, C. Agia, T. Migimatsu, M. Pavone, and J. Bohg. Text2motion: From natural language instructions to feasible plans. *Autonomous Robots*, 47(8):1345–1365, 2023.
- [20] P. Zhi, Z. Zhang, M. Han, Z. Zhang, Z. Li, Z. Jiao, B. Jia, and S. Huang. Closed-loop open-vocabulary mobile manipulation with gpt-4v. *arXiv preprint arXiv:2404.10220*, 2024.
- [21] D. Driess, F. Xia, M. S. Sajjadi, C. Lynch, A. Chowdhery, B. Ichter, A. Wahid, J. Tompson, Q. Vuong, T. Yu, et al. Palm-e: An embodied multimodal language model. *arXiv preprint arXiv:2303.03378*, 2023.
- [22] W. Huang, C. Wang, R. Zhang, Y. Li, J. Wu, and L. Fei-Fei. Voxposer: Composable 3d value maps for robotic manipulation with language models. *arXiv preprint arXiv:2307.05973*, 2023.
- [23] A. Lugmayr, M. Danelljan, A. Romero, F. Yu, R. Timofte, and L. Van Gool. Repaint: Inpainting using denoising diffusion probabilistic models. In *Proceedings of the IEEE/CVF conference on computer vision and pattern recognition*, pages 11461–11471, 2022.
- [24] X. Li, M. Zhang, Y. Geng, H. Geng, Y. Long, Y. Shen, R. Zhang, J. Liu, and H. Dong. Manipllm: Embodied multimodal large language model for object-centric robotic manipulation. *arXiv preprint arXiv:2312.16217*, 2023.
- [25] J. Liang, W. Huang, F. Xia, P. Xu, K. Hausman, B. Ichter, P. Florence, and A. Zeng. Code as policies: Language model programs for embodied control. In *2023 IEEE International Conference on Robotics and Automation (ICRA)*, pages 9493–9500. IEEE, 2023.
- [26] T. Gervet, Z. Xian, N. Gkanatsios, and K. Fragkiadaki. Act3d: 3d feature field transformers for multi-task robotic manipulation. In *7th Annual Conference on Robot Learning*, 2023.
- [27] L. Rout, A. Parulekar, C. Caramanis, and S. Shakkottai. A theoretical justification for image inpainting using denoising diffusion probabilistic models. *arXiv preprint arXiv:2302.01217*, 2023.
- [28] Z. Yang, J. Mao, Y. Du, J. Wu, J. B. Tenenbaum, T. Lozano-Pérez, and L. P. Kaelbling. Compositional diffusion-based continuous constraint solvers. *arXiv preprint arXiv:2309.00966*, 2023.
- [29] K. Chen, E. Lim, K. Lin, Y. Chen, and H. Soh. Behavioral refinement via interpolant-based policy diffusion. *arXiv preprint arXiv:2402.16075*, 2024.
- [30] P. Florence, C. Lynch, A. Zeng, O. A. Ramirez, A. Wahid, L. Downs, A. Wong, J. Lee, I. Mordatch, and J. Tompson. Implicit behavioral cloning. In *Conference on Robot Learning*, pages 158–168. PMLR, 2022.
- [31] N. M. Shafiullah, Z. Cui, A. A. Altanzaya, and L. Pinto. Behavior transformers: Cloning k modes with one stone. *Advances in neural information processing systems*, 35:22955–22968, 2022.
- [32] P. Sharma, L. Mohan, L. Pinto, and A. Gupta. Multiple interactions made easy (mime): Large scale demonstrations data for imitation. In *Conference on robot learning*, pages 906–915. PMLR, 2018.
- [33] J. Urain, N. Funk, J. Peters, and G. Chalvatzaki. Se (3)-diffusionfields: Learning smooth cost functions for joint grasp and motion optimization through diffusion. In *2023 IEEE International Conference on Robotics and Automation (ICRA)*, pages 5923–5930. IEEE, 2023.
- [34] A. Liu, M. Niepert, and G. V. d. Broeck. Image inpainting via tractable steering of diffusion models. *arXiv preprint arXiv:2401.03349*, 2023.

- [35] O. Elharrouss, N. Almaadeed, S. Al-Maadeed, and Y. Akbari. Image inpainting: A review. *Neural Processing Letters*, 51:2007–2028, 2020.
- [36] J. Ho, A. Jain, and P. Abbeel. Denoising diffusion probabilistic models. *Advances in neural information processing systems*, 33:6840–6851, 2020.
- [37] A. Brohan, N. Brown, J. Carbajal, Y. Chebotar, X. Chen, K. Choromanski, T. Ding, D. Driess, A. Dubey, C. Finn, et al. Rt-2: Vision-language-action models transfer web knowledge to robotic control. *arXiv preprint arXiv:2307.15818*, 2023.
- [38] R. Gong, X. Gao, Q. Gao, S. Shakiah, G. Thattai, and G. S. Sukhatme. Lemma: Learning language-conditioned multi-robot manipulation. *IEEE Robotics and Automation Letters*, 2023.
- [39] E. Zhang, Y. Lu, W. Wang, and A. Zhang. Language control diffusion: Efficiently scaling through space, time, and tasks. *arXiv preprint arXiv:2210.15629*, 2022.
- [40] S. E. Ada, E. Oztop, and E. Ugur. Diffusion policies for out-of-distribution generalization in offline reinforcement learning. *IEEE Robotics and Automation Letters*, 2024.
- [41] C.-F. Yang, H. Xu, T.-L. Wu, X. Gao, K.-W. Chang, and F. Gao. Planning as in-painting: A diffusion-based embodied task planning framework for environments under uncertainty. *arXiv preprint arXiv:2312.01097*, 2023.
- [42] P. Dhariwal and A. Nichol. Diffusion models beat gans on image synthesis. *Advances in neural information processing systems*, 34:8780–8794, 2021.

A Method Details

A.1 Keyframe Generation Implementation

In section 2.2, we introduce the method to generate keyframes from observations and task descriptions. In the first two steps, we ask ChatGPT4 to generate key steps and mapping them to the key points in the images. In practice, we present an example prompt to reason the key point position in the grasp pose generation task.

Prompt:

- You need to finish a robot manipulation task using a gripper hand.
- I will give you a [task description] and [multi-view images] to finish the task.
- The [task description] includes the main target and conditions, and you should consider both requirements.
- Please build a coordinate in the [multi-view images], in the front view, the bottom left is 0, and the upper right is 1. The x-axis points to the right, the y-axis points up, and the z-axis points outside. The coordinate from the other view will change according to the front view.

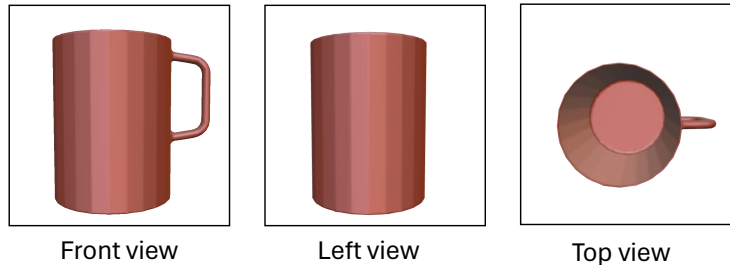
You need to:

1. According to [task description], and content in the [multi-view images], write the [key steps] to finish the task.
2. Read the [task description] and [multi-view images], and build the coordinate.
3. According to the [key steps], find the corresponding [key point] in the images. Mark the point in the front view and write the position (x,y,z) .

[task description] is: **"Pick the mug from the table to the cupboard."**

[multi-view images] are: "front view", "left view" and "top view"

Input images:



ChatGPT4 Answer:

Determine Key Steps for the Task:

1. **Approach the Mug:**
 - Use the front and left view to align the gripper with the mug.
 - Consider the height of the table and mug from the top view for z-coordinate adjustment.
2. **Grip the Mug:**
 - Adjust the gripper to the *mug's handle* dimensions primarily seen in the left view.
 - Ensure the gripper does not collide with the mug body by verifying clearance in the top view.

3. Lift the Mug:

- Elevate the gripper slowly while ensuring stability. Use top view for vertical clearance checks.

4. Transport the Mug to the Cupboard:

- Move in the x-direction (side-to-side) using the front view.
- Adjust in the z-direction (up-down) using the top view for placing inside the cupboard.

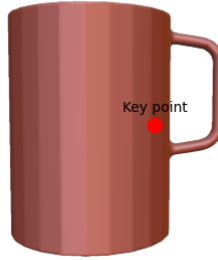
5. Release the Mug:

- Carefully open the gripper and ensure the mug is stable on the cupboard shelf.

Identify and Mark the Key Point for Gripping:

- x-coordinate: Given that the point is around 60% of the way across the width of the image.
- y-coordinate: Around 50% of the height of the image.
- z-coordinate: Since we're looking at the front view and the handle protrudes towards us.

Marked key point:



Usually, the key points can generally mark the position of conditions, but they are not the exact grasp points and are likely unreachable for the robot end-effector. Instead, We can use the key points as coarse guidance to control the policy. Finally, we obtain the key point position and calculate keyframes based on environment and policy.

A.2 Inpainting Optimization

We define the inpainting optimization problem in Eqn. (1), (2), (4) and (5), where D^{key} denotes the L-2 norm distance function. By plugging Eqn. (1) and (2) to Eqn. (4) and (5), we can simplify the optimization problem as a convex optimization as,

$$\mathbf{x}_{i-1} = \underset{\mathbf{x}_{i-1}}{\operatorname{argmin}} \sum_{k, \mathbf{m}^{[k]}=1} \left(\mathbf{x}_{i-1}^{[k]} - \mathbf{x}_{i-1}^{\text{known}, [k]} \right)^2 \quad (6)$$

$$\text{s.t. } \frac{1}{2} [\mathbf{x}_{i-1} - \mu_{\theta}(\mathbf{x}_i, i)]^T \Sigma_{\theta}^{-1}(\mathbf{x}_i, i) [\mathbf{x}_{i-1} - \mu_{\theta}(\mathbf{x}_i, i)] \leq \gamma'_{i-1} \quad (7)$$

$$\gamma'_i = \gamma_i - \frac{1}{2} \log [(2\pi)^d \Sigma_{\theta}(\mathbf{x}_i, i)] \quad (8)$$

where superscript $[k]$ denotes the k_{th} element of the vector. d denotes the dimension of the actions. γ'_i is the normalized constraint based on γ_i and covariance matrix.

B Simulation Environments

In the simulation environments, we designed specific settings for "Push-T", "Block-push", "Franka Kitchen" and "grasp pose" to test our diffusion policy and inpainting methods under various task conditions.

Push-T: A blue round end-effector pushes a gray T-block towards a fixed green T-shaped target. Successful task completion is based on the alignment between the T-block and the target. The end-effector starts from the target's top-right, while the T-block starts from the bottom-left, each with random positional and rotational deviations. The task descriptions involve detouring the block from specified sides (left, right, top, down), with unseen conditions being TOP and DOWN due to the lack of demonstration trajectories from these directions, which may cause the policy to fail by colliding with the block.

Block-Push: This involves pushing red and green blocks into designated target squares, structured in two phases—moving one block followed by the other. Random deviations in initial positions introduce unpredictability in successful trajectories. Demonstrations exist for prioritizing either block, forming the basis for task descriptions that dictate the order of operations. Unseen tasks include non-existent color blocks to test the algorithm's response to erroneous instructions and open-vocabulary tasks that challenge the system's interpretative flexibility.

Franka Kitchen: Comprising seven sub-tasks grouped into three levels based on their locations, this environment tests the robot arm's ability to perform sequential tasks as specified by the task descriptions. All single tasks are seen during demonstrations, making them familiar, while multiple tasks involve unseen sequences, especially when changing from high to mid or low levels, or vice versa, challenging the policy's adaptability.

Grasp Pose Generation: This environment focuses on the precise task of generating grasp poses for four different objects: mugs, bottles, hammers, and forks. Each object has associated tasks, divided into seen and unseen categories, where the seen tasks involve specific, demonstrated grasping actions, and the unseen tasks introduce new, potentially open-vocabulary or challenging conditions.

Table 2: Language Task Descriptions for Different Environments

Environment	Seen Tasks	Unseen Tasks
Push-T	<ul style="list-style-type: none"> • Push the block to the target region and detour from LEFT side. • Push the block to the target region and detour from RIGHT side. 	<ul style="list-style-type: none"> • Push the block to the target region and detour from TOP side. • Push the block to the target region and detour from DOWN side.
Block-push	<ul style="list-style-type: none"> • Push the RED block to the target, then the GREEN block to its target. • Push the GREEN block to the target, then the RED block to its target. 	<ul style="list-style-type: none"> • Push the YELLOW block to the target, then the BLUE block to its target. • Push two blocks to targets in any sequence.
Franka Kitchen single-task	<ul style="list-style-type: none"> • Complete task A. (A is one of the sub-tasks in the Kitchen environment.) 	-
Franka Kitchen multi-task	<ul style="list-style-type: none"> • Complete task A, then task B. (Demonstrations have trajectories with A to B order.) 	<ul style="list-style-type: none"> • Complete task C, then task D. (Demonstrations do not have trajectories in C to D order.)
Grasp Pose: Mug	<ul style="list-style-type: none"> • Grasp the mug RIM (top). • Grasp the mug HANDLE. 	<ul style="list-style-type: none"> • Give me the mug. • Grasp the mug BOTTOM.
Grasp Pose: Bottle	<ul style="list-style-type: none"> • Grasp the bottle on LEFT side. • Grasp the bottle on RIGHT side. 	<ul style="list-style-type: none"> • LIFT the bottle. • Grasp the bottle BOTTOM.
Grasp Pose: Hammer	<ul style="list-style-type: none"> • Grasp the hammer HANDLE. • Grasp the hammer HEAD. 	<ul style="list-style-type: none"> • USE the hammer. • HAND OVER the hammer.
Grasp Pose: Fork	<ul style="list-style-type: none"> • Grasp the fork HANDLE. • Grasp the fork HEAND. 	<ul style="list-style-type: none"> • PICK up the fork. • HAND OVER the fork.

The environment is designed to test the diffusion policy’s ability to adapt its output (a 6D grasp pose) based on the conditions provided by the task descriptions. Keyframes are generated from the positions in 3D space, which guide the policy in generating actions conditioned by the specific grasp requirements. The key point here is the direct application of conditions to the action generation through inpainting, which does not involve temporal sequencing but rather focuses on spatial accuracy and relevance.

Each environment utilizes a diffusion policy where actions are determined by the 2D or 3D positions of keyframes generated via vision-language models. This setup tests both the precision of task execution based on seen instructions and the flexibility of the system under unseen or open-vocabulary conditions. The task descriptions for each environments are listed in Table 2.

C Real-robot Experiment Details

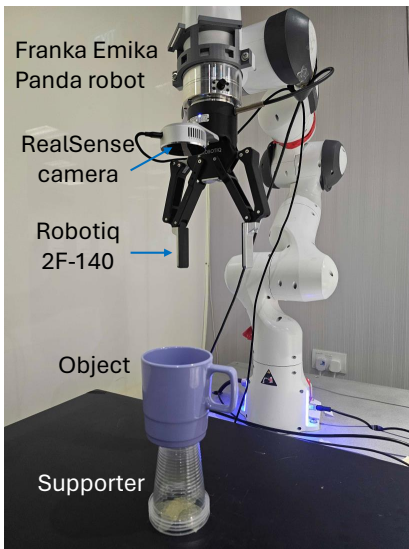


Figure 7: Real-robot experiment setup.

The real robot experiments adopted the Franka Emika robot to grasp and manipulate different objects according to task descriptions. The RealSense camera observed the multi-view RGB-D images and generated point clouds as observation. The end-effector was the Robotiq 2F-140 gripper. A supporter was placed to lift the objects, which enlarged the workspace of the robot arm. We filtered out the supporter in the point cloud. For each object, we transferred the trained model in simulation to the real robot and sampled 10 grasps for seen and unseen task (Table 2).

One big challenge in the real-world experiment was the partial observation of the point cloud. Unlike point clouds sampled from simulated meshes, the camera-generated point clouds had an uneven density over different regions. For example, the mug handle has a sparser point cloud density than the rim. This problem led to a strong Sim2Real gap and failures of fine-tuned conditional models.

D Networks, Datasets and Training Details

For simulation experiments, we adapted the program from [2] for push-T, push-block and Franka kitchen environments; and used the [33] for grasp pose generation environments. For diffusion policy networks that predict action sequences, we adopted the transformer-based backbone for state-based environments. For inpainting optimization, we formulated the convex optimization problem and utilized CVXPY to obtain the optimal solutions. We built the language-conditioned classifier network with text as input, followed by tokenization and encoding [14]. For the goal-conditioned classifier network, we augmented the network inputs with the normalized goal state [13]. Finally, we trained the classifier guidance networks to control the generation of diffusion models [42].

The training datasets were adapted from [2] and [33]. We filtered and labeled the demonstrations with task descriptions for each environment. Note that in our experiments, we only used demonstrations that corresponded to pre-defined task descriptions and neglected other trajectories. In addition, we marked the terminal state of each trajectory as the goal state for goal-conditioned networks. For continuous action environments, we used batch size = 256, and for the grasp pose (single-action) en-

vironment, batch size = 2. We trained networks in our local personal computer, that the CPU model is Intel(R) Core(TM) i9-14900KF and the GPU model is RTX 4090. During the training process, the average GPU memory usage is 12GB. The average training time for the diffusion model was 8 ~ 10 hours.